INL/CON-08-14622
PREPRINT

Idaho National Laboratory Experimental Research in High Temperature Electrolysis for Hydrogen and Syngas Production

ASME 4th International Topical Meeting on High Temperature Reactor Technology

Carl M. Stoots
James E. O'Brien
J. Stephen Herring
Keith G. Condie
Joseph J. Hartvigsen

September 2008

Idaho National
Laboratory

Proceedings of HTR2008
Fourth International Topical Meeting on High Temperature Reactor Technology
September 28 – October 1, 2008, Washington D.C., USA

HTR2008-58086

IDAHO NATIONAL LABORATORY EXPERIMENTAL RESEARCH IN HIGH TEMPERATURE ELECTROLYSIS FOR HYDROGEN AND SYNGAS PRODUCTION

Carl M. Stoots
Idaho National Laboratory
Idaho Falls, ID, USA

James E. O'Brien
Idaho National Laboratory
Idaho Falls, ID, USA

J. Stephen Herring
Idaho National Laboratory
Idaho Falls, ID, USA

Keith G. Condie
Idaho National Laboratory
Idaho Falls, ID, USA

Joseph J. Hartvigsen
Ceramatec, Inc.
Salt Lake City, UT, USA

ABSTRACT

The Idaho National Laboratory (Idaho Falls, Idaho, USA), in collaboration with Ceramatec, Inc. (Salt Lake City, Utah, USA), is actively researching the application of solid oxide fuel cell technology as electrolyzers for large scale hydrogen and syngas production. This technology relies upon electricity and high temperature heat to chemically reduce a steam or steam / CO_2 feedstock. Single button cell tests, multi-cell stack, as well as multi-stack testing has been conducted. Stack testing used 10 x 10 cm cells (8 x 8 cm active area) supplied by Ceramatec and ranged from 10 cell short stacks to 240 cell modules. Tests were conducted either in a bench-scale test apparatus or in a newly developed 5 kW Integrated Laboratory Scale (ILS) test facility. Gas composition, operating voltage, and operating temperature were varied during testing. The tests were heavily instrumented, and outlet gas compositions were monitored with a gas chromatograph. The ILS facility is currently being expanded to ~15 kW testing capacity (H_2 production rate based upon lower heating value).

INTRODUCTION

Conventional world oil production will eventually peak and subsequently decline. Predictions of when this peak will occur are controversial and difficult to make due to geological complexities, measurement problems, pricing variations, demand elasticity, and political influences [1]. However, the impact of peak oil could be tremendous and unprecedented. In the present, demands upon existing reserves and production capacity are growing, primarily due to industrializing nations such as China and India [2]. These issues plus recent escalations in crude oil prices, shrinking new discoveries, and worries over crude supply disruptions have made energy security an important topic. Finally, there are the climate change aspects of oil usage. Most of the United State's energy-related CO_2 emissions come from oil.

These developments have created a strong interest in developing hydrogen as a second energy carrier for the non-electrical energy market. Water-splitting for hydrogen production can be accomplished via high-temperature electrolysis or thermochemical processes, using high-temperature nuclear process heat and electricity. In order to achieve competitive efficiencies, both processes require high-temperature operation. High-temperature electrolytic water-splitting supported by nuclear process heat and electricity has the potential to produce hydrogen with an overall system efficiency near those of the thermochemical processes [3], but without the corrosive conditions of thermochemical processes and without the fossil fuel consumption and greenhouse gas emissions associated with hydrocarbon processes. The Idaho National Laboratory (INL), in conjunction with Ceramatec Inc. (Salt lake City, USA) has been researching the use of solid-oxide fuel cell technology to electrolyze steam for large-scale nuclear-powered hydrogen production. The scope of activities includes computational fluid dynamics modeling, process flow sheet analyses, and experimental testing. Scales of experimental testing have progressed from ~2 watt button cell tests to 5 kW multi-stack tests. The INL is now constructing a 15 kW high temperature electrolysis test facility, to be operable in September, 2008.

It is recognized, however, that the conversion of the present liquid hydrocarbon transportation fuel infrastructure to hydrogen will require decades. In the interim, domestically produced synthetic hydrocarbon fuels (synfuels) can serve as a bridge to an ultimate hydrogen economy. The feedstock for synfuel production is hydrogen and carbon monoxide (syngas). Traditionally, syngas has been produced via coal gasification, and more recently by steam reforming of natural gas. Both techniques consume non-renewables and emit greenhouse gases.

The INL, again in collaboration with Ceramatec Inc., has also been studying the extension of high temperature solid-oxide based steam electrolysis to the coelectrolysis of steam and carbon dioxide to produce syngas:

$$H_2O + CO_2 \xrightarrow{electricity, heat} \underbrace{H_2 + CO}_{syngas} + O_2 . \quad (1)$$

Coelectrolysis is a significantly more complicated process than steam electrolysis, and is not completely understood. It has not been shown conclusively that coelectrolysis of steam and CO_2 actually proceeds by electrolysis of both CO_2 and H_2O, or whether steam is electrolyzed predominantly or even exclusively to produce hydrogen that immediately reacts with CO_2 to produce CO via the reverse shift reaction (RSR):

$$CO_2 + H_2 \leftrightarrow CO + H_2O. \quad (2)$$

Fuel cell testing at Ceramatec in the early 1990's showed that the area specific resistance (ASR) of SOFC button cells operating on a dry CO-CO_2 feed was a factor of 10 greater than for the same cell operating with humidified hydrogen (i.e. H_2-H_2O). Electrode materials and structure development over the past 15 years at Ceramatec have closed the performance gap such that cell ASR is now only about 100%-200% greater for dry carbon dioxide electrolysis than steam electrolysis. This result has been shown in single cell testing at Ceramatec, and in 10 cm cell stack testing at INL. However, with the introduction of even a small amount of steam or hydrogen to a predominantly CO-CO_2 reactant stream, the cell performance is virtually identical to that of the cell on H_2-H_2O alone.

Regardless of the mechanism, the practical implication is that coelectrolysis is preferred to dry electrolysis of CO_2. An even more important reason that dry CO_2 electrolysis is not recommended is because under most conditions the reduction potential of CO to solid carbon is only slightly higher than for CO_2 to CO. Under conditions of high CO_2 conversion, the reduction potential of CO actually becomes less than that of CO_2 making carbon deposition difficult to avoid. In coelectrolysis, CO concentrations are decreased by the presence of steam and hydrogen, such that carbon deposition by electrochemical reduction of CO is not generally possible.

This paper offers a summary of the INL/Ceramatec experimental activities to date on high temperature electrolysis for hydrogen and syngas production, with facility descriptions and future plans. Sample experimental results are presented that summarize electrolysis performance at various temperatures, gas mixtures, and electrical settings. For coelectrolysis, product gas compositions as measured via an online micro gas chromatograph (GC) are compared to predictions obtained from an INL-developed chemical equilibrium coelectrolysis model (CECM). An inline methanation reactor has also been tested to study direct methane production from coelectrolysis products.

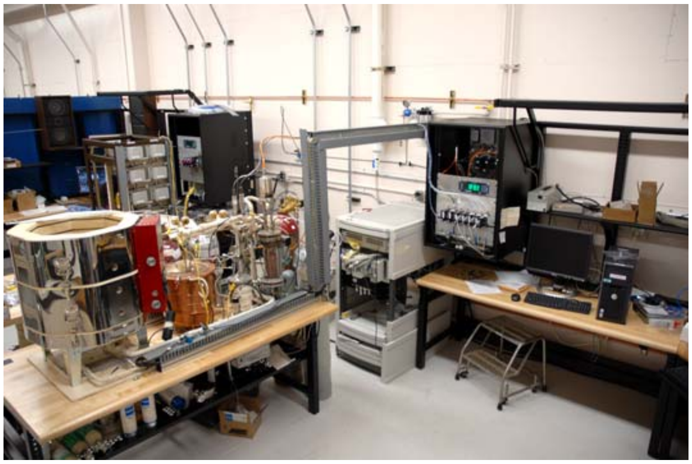

Fig. 1. INL high-temperature electrolysis laboratory.

The ILS facility has been designed for an ultimate nominal hydrogen production rate of 14.1 kW based on lower heating value (LHV, equal to 120 MJ/kg for hydrogen) [4], or 4735 Normal (273°K, 1 atm) L/hr. The initial ILS facility single module implementation was designed for ~5 kW hydrogen production. Neither heat recuperation nor hydrogen recycle were incorporated. The facility is now being expanded to handle 3 solid oxide modules for a total of 720 64 cm^2 cells. Limited heat recuperation as well as hydrogen recycle is being included as well. The use of recuperation minimizes the net heat addition required to heat the process gas streams up to the high temperature electrolysis (HTE) operating temperature.

When linked to nuclear power, high temperature electrolysis can offer a carbon-free means for large scale H_2 production while coelectrolysis can provide a carbon neutral means of producing syngas while consuming CO_2.

CURRENT EXPERIMENTAL TESTING FACILITY

A comprehensive discussion of the INL high temperature solid oxide electrolysis bench scale experiment is presented elsewhere [5, 6]. This same facility is used for button cell testing as well as stack testing. A photograph of the test hardware is found in Figure 1 and a schematic follows in Figure 2. Primary components include gas supply cylinders, mass-flow controllers, a humidifier, dewpoint measurement stations, carbon dioxide concentration measurement stations, microchannel gas chromatograph, temperature and pressure measurement, high temperature furnace, and a solid oxide electrolysis cell. Nitrogen is used as an inert carrier gas. The use of a carrier gas allows for independent variation of both the partial pressures and the flow rates of the inlet steam, hydrogen, and CO_2 gases while continuing to operate near atmospheric pressure. The flow rates of nitrogen, hydrogen and air are established by means of precision mass-flow

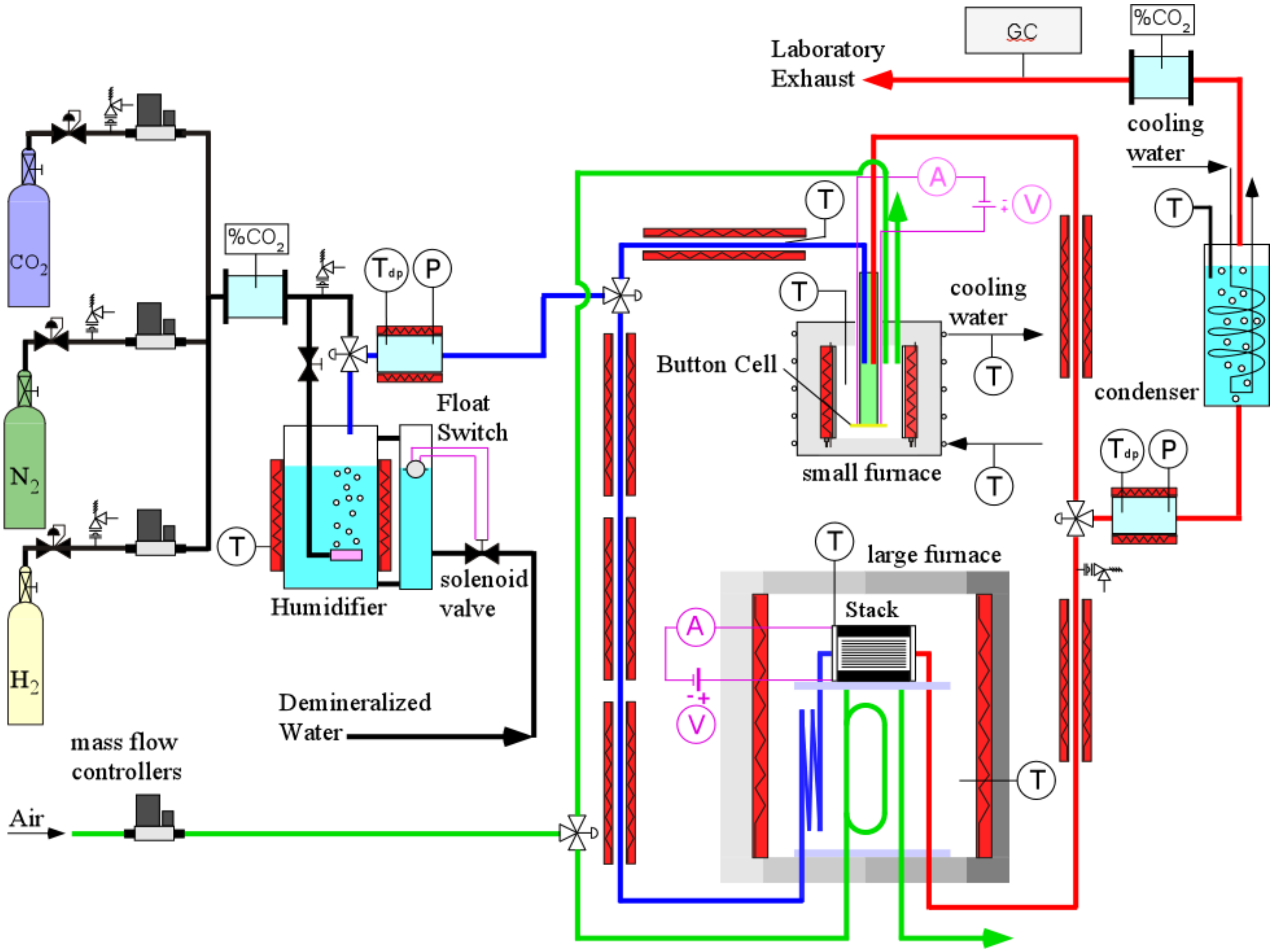

Fig. 2. Schematic of INL electrolysis / coelectrolysis bench-scale test apparatus.

controllers. Air flow to the stack is supplied by the shop air system, after passing through a two-stage extractor / dryer unit.

Downstream of the mass-flow controllers, nitrogen is mixed with smaller flows of hydrogen gas and CO_2. Hydrogen is included in the inlet flow as a reducing gas in order to prevent oxidation of the Nickel cermet electrode material. The nitrogen / hydrogen / CO_2 gas mixture is mixed with steam by means of a heated humidifier. The humidifier water temperature is maintained at a constant setpoint value using computerized feedback control. The dewpoint temperature of the nitrogen / hydrogen / CO_2 / steam gas mixture exiting the humidifier is monitored continuously using a precision dewpoint sensor. Pressure is also measured at the dewpoint measurement stations using absolute pressure transducers. Local stream pressure information is required to determine the mole fraction of steam in the gas mixture at the dew point measurement station. Since the nitrogen, hydrogen, and CO_2 flow rates are fixed by the mass flow controllers, and the steam partial pressure is fixed by the bath temperature, the complete inlet gas composition is precisely known at all times. All gas lines located downstream of the humidifier are heat-traced in order to prevent steam condensation. Gas line temperatures are monitored by thermocouples and controlled by means of computer-controlled SCRs.

The electrolysis product stream exiting the furnace is directed towards a second dewpoint sensor and a CO_2 sensor upon exiting the furnace and then to a condenser through a heat-traced line. The condenser removes most of the residual steam from the exhaust. The final exhaust stream is vented outside the laboratory through the roof.

The rates of steam and CO_2 electrolysis are measured via three different, independent methods: 1) electrical current through the stack, 2) the measured change in inlet and outlet steam and CO_2 concentrations as measured by the on-line dew point and CO_2 sensors, and 3) an on-line microchannel GC. The GC also tests for any additional electrolysis products, such as CH_4, that may be produced.

For single-cell testing, an electrolysis button cell is bonded to the bottom of a zirconia tube. During testing, the tube is suspended in the smaller furnace. The cell is an electrolyte-supported single button cell with a scandia-stabilized zirconia electrolyte, about 150 µm thick. The outside electrode, which acts as the cathode in fuel cell mode and the anode in electrolysis mode, is a doped manganite. The inside electrode (electrolysis cathode) material is a nickel cermet. Both button-cell electrodes incorporate a platinum wire mesh for current distribution. The button cell includes both an active cell area ($2.5\ cm^2$ for the cell shown) and a reference cell area. A type-K stainless-steel sheathed thermocouple is mounted on the manifold tube and bent around in front of the button cell in order to allow for continuous monitoring of the button-cell temperature.

For stack testing, the inlet gas mixture is directed to the larger high temperature furnace, which heats and maintains the electrolyzer at the appropriate test temperature via computer-based feedback control. The furnace also preheats the inlet gas mixture and the air sweep gas. A photograph of the stack, mounted on its inconel test fixture and resting on the furnace base, is shown in Figure 3. The button cells and stacks were fabricated by Ceramatec, Inc., of Salt Lake City, UT. The stacks have a per-cell active area of 64 cm2, for a total active area of 640 cm2 each.

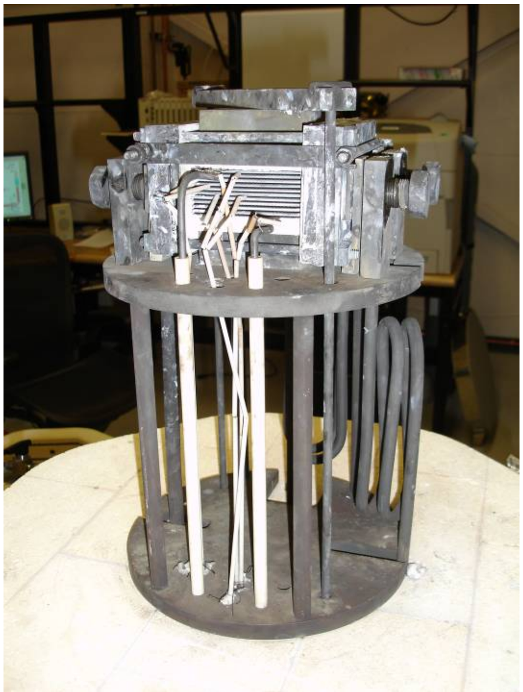

Fig. 3. 10-cell stack mounted on test fixture on furnace base, ready to test.

The piping and instrumentation schematic for the ILS single-module experiment with no heat recuperation or hydrogen recycle is shown in Figure 4. A photograph of the ILS skid with the components identified is presented in Figure 5. The components are listed in Table I by identification number. The ILS facility is currently being expanded to accommodate three modules as well as heat recuperation and hydrogen recycle. The electrolysis module requires a support system supplying electrical power for electrolysis, a feedstock gas mixture of hydrogen and steam, a sweep gas, and appropriate exhaust handling. In particular, this system must include means for controlled steam generation, mixing hydrogen with the steam, feedstock and product dewpoint measurements, heating the feedstock and sweep gas to the appropriate electrolysis temperature (via a superheater), cooling the electrolysis product stream, condensing any residual steam out of the product stream, and venting the hydrogen product. The final ILS support system will consist of three parallel systems that supply feedstock, sweep gas streams, and electrical power basically independent of each other to each of three modules. All three modules will be located within a

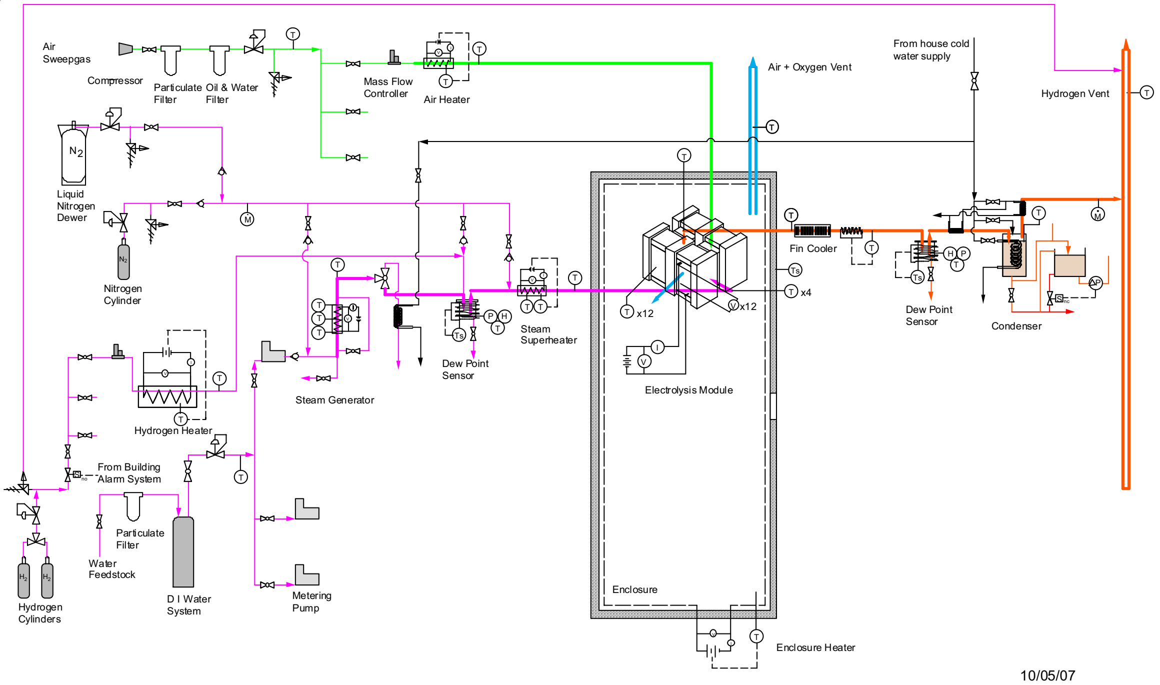

Fig. 4. ILS single module piping and instrumentation schematic.

Fig. 5. INL ILS facility, with major components labeled.

TABLE I
Component identifiers for Figure 6.

ID	Component
1	Electrolysis stacks / module
2	Hot zone enclosure lid
3	Power supply and instrument racks
4	Electrical distribution cabinets
5	Data acquisition and control monitors
6	Deionized water system
7	Water supply metering pump
8	Steam generator
9	H_2 preheater
10	Steam and H_2 superheater
11	Air compressor
12	Air heater
13	Product finned cooler
14	Steam condenser
15	Condensate tank
16	H_2 mass flow meter
17	H_2 vent
18	Air and O_2 vent
19	Dew point sensor

single hot zone. The facility is designed to accommodate later incorporation of heat recuperation and hydrogen recycle capabilities. To aid in interpretation of Figure 4, the hydrogen / steam feedstock is represented by the color magenta, the product stream by orange, the inlet sweep gas by green, and the outlet sweep gas by blue.

Liquid water feedstock is fed at a controlled rate into the system by means of a positive-displacement metering pump. The water is then vaporized and slightly superheated in an inline electrically-powered steam generator. The steam generator was fabricated by attaching a combination of fifteen 200 and 300 watt clamp-on electric heaters to the outside of a 1” diameter stainless steel tube. The heaters are covered with 2” of thermal insulation, then topped by an aluminum covering. The heaters are spaced such that a higher heat flux is obtained in the boiling region and lower heat flux in the single-phase regions. The heaters are all wired in parallel so that each operates at the same voltage. The tube interior is filled with a copper foam material which reduces flow perturbations and increases temperature uniformity in the boiling region. The outlet temperature is controlled by carefully adjusting the input power supplied by a DC power supply to obtain the desired superheat temperature.

The slightly superheated steam exiting the steam generator is mixed with hydrogen, which is required on the inlet side of the stack in order to maintain reducing conditions at the steam/hydrogen electrode. In the initial ILS configuration (prior to the implementation of hydrogen recycle), the inlet hydrogen is supplied from a compressed gas bottle. The hydrogen flow rate is controlled by a mass-flow controller and the data acquisition / control system (DACS). The inlet hydrogen must be heated to the steam generator outlet temperature in order to prevent cooling of the steam and possible steam condensation. This is accomplished by temperature-based feedback control of the hydrogen preheater powered by a DC power supply in conjunction with the DACS. Downstream of the mixing point, the temperature, pressure, and dewpoint of the steam/hydrogen gas mixture are measured. The absolute pressure is directly measured at the dewpoint measurement station in order to allow for accurate determination of the steam mole fraction. Precise measurement of the dewpoint and pressure allows for independent determination of the inlet gas composition.

A high-temperature electrically powered inline superheater then boosts the feedstock stream to the final electrolyzer operating temperature, 800° - 830°C. Heat is supplied from six semi-cylindrical ceramic-fiber heaters with embedded coiled elements. Each heater section is capable of providing 1800 watts of power when operated at 240 volts, but they are operated at a much lower voltage for this application. Power is supplied to the heaters from 3.3 kW DC power supplies. Heater power is feedback-controlled based on thermocouples located inside the ceramic fiber heaters. Two inch thick high-temperature thermal insulation is wrapped around the heaters and covered with an aluminum skin.

The primary material of construction for the low-temperature tubing and components upstream of the superheater is 316 stainless steel. For high temperatures such as 800°C, Inconel 600 tubing is used within the superheater and air heater.

The electrolysis module is mounted in the hot zone enclosure where it is maintained at the desired operating temperature using radiant heaters installed in the sides and top of the removable lid. As explained in reference [5], when the electrolysis process is operated below the thermal neutral voltage (voltage at which stack ohmic heating balances the endothermic heat requirement, V_{tn} = 1.287 V/cell for 800°C operating temperature), heat must be added to overcome the endothermic reaction heat requirement. At thermal neutral conditions, the module operation is adiabatic and isothermal. If, however, the module is operated above the thermal neutral voltage, heat must be removed from the system.

The base of the hot zone enclosure consists of a stainless steel plate covered with several inches of high-temperature insulation. The module rests on top of the insulation. The process streams, power leads, and instrumentation access the module through holes in the bottom plate and insulation. A stainless-steel lid covers the hot zone enclosure and is sealed against the bottom plate with an O-ring. The radiant heater panels are powered by a DC power supply, feedback-controlled based on a thermocouple mounted inside the enclosure. The lid is attached to screw-drive rods on each end, driven by an electric motor, which allow for convenient raising and lowering of the lid.

The gas mixture exiting the electrolyzer will be significantly enriched in hydrogen, typically to at least 50% hydrogen mole fraction, with the remainder being residual steam. The product stream is first cooled via a natural-convection air-cooled heat exchanger. The product stream temperature exiting this cooler is controlled such that no condensation can occur. Then the product gas mixture enters the outlet dewpoint measurement station. As discussed previously, the measurement of both inlet and outlet dewpoint temperatures allows for direct determination of the steam consumption rate, and the corresponding hydrogen production rate. This rate can be compared to the electrochemical hydrogen production rate determined from the stack electrical current. The outlet hydrogen/steam flow then enters a condenser where the vast majority of the residual steam is removed. The rate of water condensation is monitored via tank level, providing an additional independent measure of steam consumption. At this point, the product stream will be ambient-temperature, saturated hydrogen gas, with about 2.7% residual water vapor. The flow rate of this product gas is measured with a low-pressure-drop mass flow transducer. Comparison of the condensate and hydrogen product mass flow rates with the electrolyzer inlet mass flow rates helps quantify any stack leakage that may occur. The hydrogen product is then vented from the building.

Air is used as a sweep gas to remove oxygen produced by the ILS system. Filtered compressed air flows through a mass-flow controller and into an electrically-powered heater to preheat the inlet air to the stack operating temperature. Downstream of the electrolyzer, the hot oxygen-enriched air stream is then vented from the building to the environment.

Nitrogen gas can be injected directly into the steam superheater. This feature is used during startup until the superheater outlet temperature reaches about 400ºC to preclude any liquid entering the electrolysis module. During some scenarios, nitrogen gas may continue to be injected during steady state operation. For instance, if a module is found to be particularly leaky, nitrogen can be used to increase the average molecular weight of the gas mixture and hence reduce hydrogen diffusion rates. The nitrogen can be supplied from either a compressed gas cylinder or from a liquid nitrogen Dewar.

Detailed process flow sheets were developed for the ILS design using the commercial system-analysis code UniSim. These flow sheets include all of the components present in the actual ILS facility such as pumps, heaters, condensers, and the electrolyzer. Since the electrolyzer is not a standard UniSim component, a custom one-dimensional electrolyzer model was developed for incorporation into the overall process flow sheet. This electrolyzer model allows for the determination of the H_2 production rate, average Nernst potential, cell operating voltage, gas outlet temperatures, and electrolyzer efficiency for any specified inlet steam, hydrogen, and sweep-gas flow rates, current density, cell active area, and external heat loss or gain. The model includes a temperature-dependent area-specific resistance (ASR) that accounts for the significant increase in electrolyte ionic conductivity that occurs with increasing temperature. Details concerning this one-dimensional model and its implementation in UniSim have been reported in [5, 7].

All of the system components and hardware were mounted on a skid that is 16 ft. long by 10 ft wide. A custom LabView (National Instruments) program was developed for ILS data acquisition and instrument control using SCXI data acquisition hardware.

ELECTROLYSIS STACKS AND MODULES

Planar stacks used for testing by the INL are fabricated by Ceramatec, Inc., of Salt Lake City, UT. The internal components of the stack are shown in Figure 6 and are comprised as follows. The interconnect plate is fabricated primarily from ferritic stainless steel. It includes an impermeable separator plate (~0.46 mm thick) with edge rails and two corrugated flow fields, one on the sweep-gas side and one on the steam / hydrogen side. The height of the flow fields is 1.0 mm. Each flow field includes 32 perforated flow channels across its width to provide uniform gas-flow distribution. The steam / hydrogen flow fields are fabricated from nickel foil. The air-sweep flow fields are made from ferritic stainless steel. The interconnect plates and flow fields also serve as electrical conductors and current distributors. To improve performance, the sweep-side separator plates and flow fields are surface-treated to form a rare-earth stable conductive oxide scale. A perovskite rare-earth coating is also applied to the separator plate oxide scale by either screen printing or plasma spraying. On the steam / hydrogen side of the separator plate, a thin (~10 μm) nickel metal coating is applied.

The electrolyte is scandia-stabilized zirconia, ~140 μm thick. The sweep-side electrode (anode in the electrolysis mode) is a strontium-doped manganite. The electrode is graded, with an inner layer of manganite/zirconia (~13 μm) immediately adjacent to the electrolyte, a middle layer of manganite (~18 μm), and an outer bond layer of cobaltite. The steam / hydrogen electrode (cathode in the electrolysis mode) is also graded, with a nickel cermet layer (~13 μm) immediately adjacent to the electrolyte and a pure nickel outer layer (~10 μm).

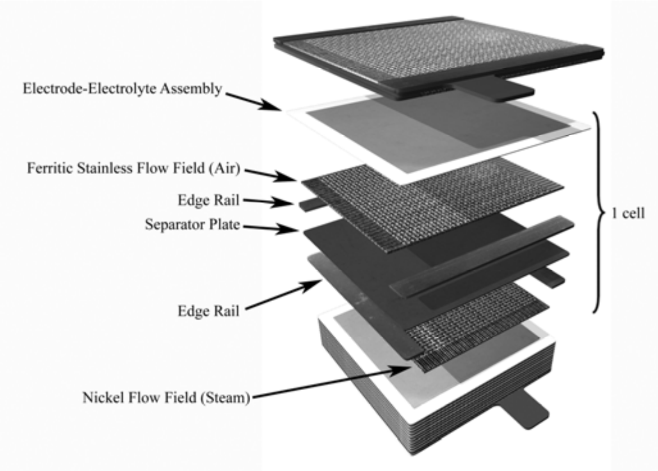

Fig. 6. Diagram of solid-oxide stack components.

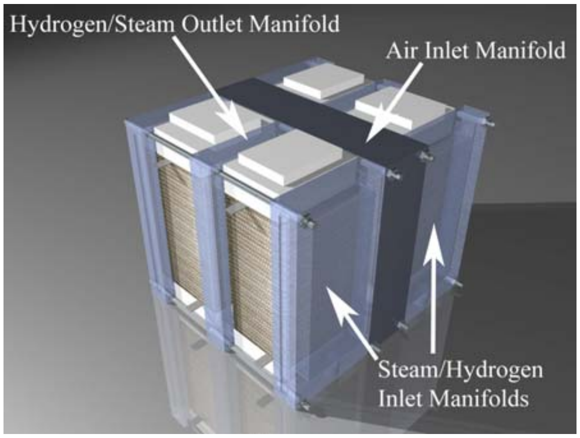

Fig. 7. ILS 4-stack module.

In the INL ILS facility, four sixty-cell stacks are combined into a module (see Figure 7). Each cell has an active area of 64 cm^2 per cell, providing a total active area of 15,360 cm^2 in a module. They are designed to operate in cross flow, with the steam / hydrogen gas mixture entering the inlet manifolds on the right and left sides, and exiting through the outlet manifold visible in Figure 7. Airflow enters through an air inlet manifold (Figure 7) and exits through the front and back open faces directly into the hot zone enclosure.

Each pair of stacks is called a half module (Figure 8). To preclude the loss of an entire stack if a single cell fails, the four stacks are electrically interconnected at every fifth cell. This is done by first electrically interconnecting the pair of stacks in each half module (Figure 8), and then interconnecting the two half modules when they are in final position. When the two half-modules are positioned, a common air inlet plenum for all four stacks is formed. Spring loaded bars are placed over the stacks to maintain a compressive load on the stacks during operation. Power leads to each stack, intermediate voltage taps

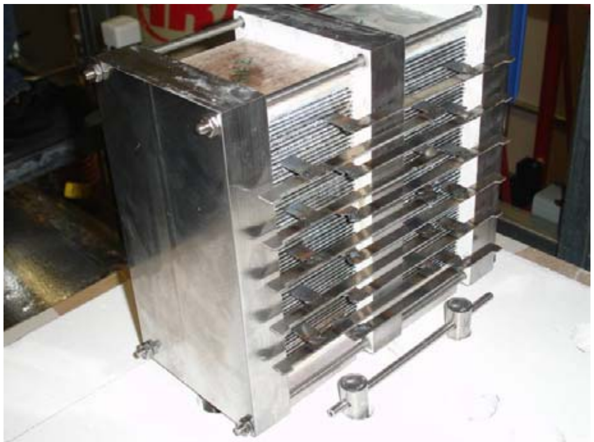

Fig. 8. One-half of ILS module showing electrical interconnections.

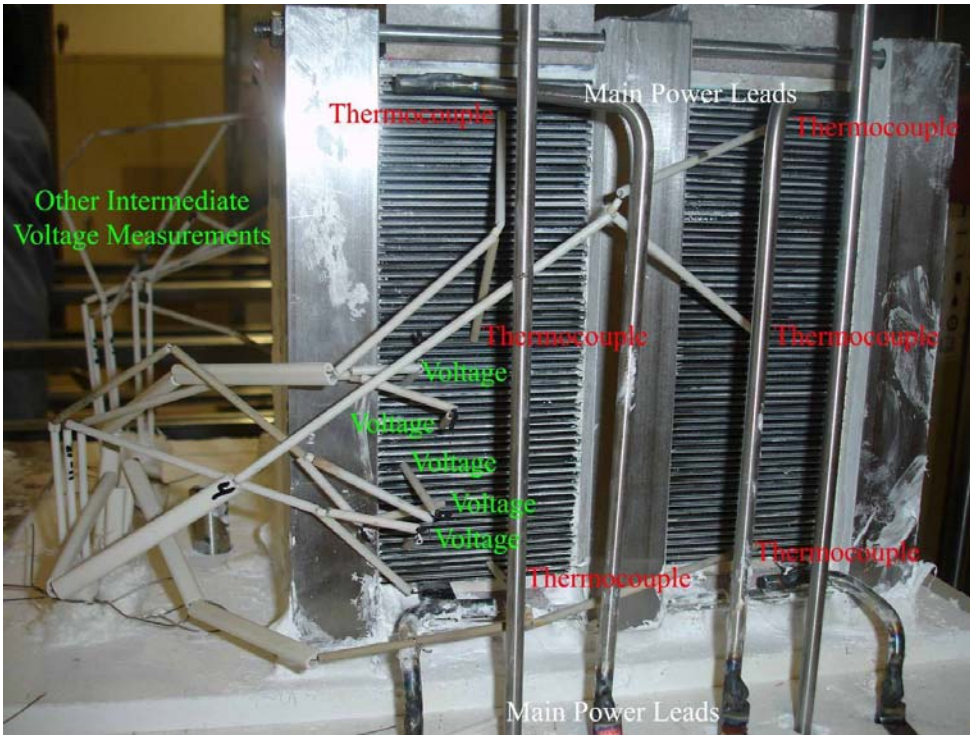

Fig. 9. Final installation of ILS module with instrumentation and power attachments.

and interior thermocouples were then attached, and subsequent sealing of gaps completed the installation (Figure 9).

A summary of the operating parameters and nominal predicted performance characteristics of the ILS for one module is provided in Table II. Three modules will be incorporated in the final ILS configuration, each of which will include 4 stacks of 60 cells each, totaling 720 cells. The nominal performance of the 3-module system can be scaled from Table II.

TABLE II.

ILS single module design parameters.

Independent Design and Operational Parameters	
active cell area	64 cm^2
cells per stack	60
number of stacks	4
stack operating temperature	830°C
steam utilization	50%
stack operating voltage	77 V
per-cell ASR	1.5 Ωcm^2
inlet steam mole fraction	0.9
inlet hydrogen mole fraction	0.1
Anticipated Performance Values	
per-cell operating voltage	1.283 V
current density	0.25 A/cm^2
stack power	1232 W
total power (electric)	4.85 kW
inlet hydrogen flow rate	5.8 NLPM
inlet steam flow rate	53 NLPM
inlet liquid water flow rate	0.7 g/s
air flow rate	22.6 NLPM
hydrogen production rate	1578 NL/hr
heating value of hydrogen produced	4.7 kW (LHV)

COELECTROLYSIS CHEMICAL EQUILIBRIUM MODEL

A chemical equilibrium coelectrolysis model was developed to provide a predictive capability for coelectrolysis testing. This model also served to help determine the necessary inlet conditions for the range of experiments that were conducted.

The open-cell potential for the coelectrolysis system can be calculated as a function of temperature using the Nernst equation for either steam-hydrogen or for CO_2-CO, provided the equilibrium composition of the components is used in the evaluating the equation. Therefore, the equilibrium composition must be determined first, by any appropriate method.

The overall shift reaction can be represented as:

$$a_0 + b_0 + c_0 + d_0 \rightarrow a_1 + b_1 + c_1 + d_1 \tag{3}$$

where a_0, b_0, c_0, and d_0 represent the cold inlet mole fractions of CO, CO_2, H_2, and H_2O, respectively, that are known from the inlet gas flow rate and dewpoint measurements. The unknown equilibrium mole fractions of the four species at the electrolyzer temperature, prior to electrolysis, are represented by a_1, b_1, c_1, and d_1. The three corresponding chemical balance equations for carbon, hydrogen, and oxygen are:

$$a_0 + b_0 = a_1 + b_1 \tag{4}$$

$$2c_0 + 2d_0 = 2c_1 + 2d_1 \qquad (5)$$

$$a_0 + 2b_0 + d_0 = a_1 + 2b_1 + d_1 . \qquad (6)$$

To complete a system of four equations and four unknowns, the equilibrium constant for the shift reaction:

$$k_{RSR}\left(T\right) = \frac{b_1 c_1}{a_1 d_1} \qquad (7)$$

is included.

Using a correlation for the reverse gas shift reaction equilibrium constant as a function of gas temperature and the room temperature inlet gas molar composition, the model calculates the equilibrium gas composition as the inlet gas mixture heats up to electrolysis conditions (800 to 830°C). Once the hot equilibrium composition is determined, the Nernst potential can be calculated from:

$$\begin{aligned} V_N &= \frac{-\Delta G_{f,H_2O}(T)}{2F} - \frac{R\,T}{2F}\ln\left[\left(\frac{d_1}{c_1 y_{O2}^{1/2}}\right)\left(\frac{P}{P_{std}}\right)^{-1/2}\right] \\ &= \frac{-\Delta G_{f,CO_2}(T)}{2F} - \frac{R\,T}{2F}\ln\left[\left(\frac{d_1}{c_1 y_{O2}^{1/2}}\right)\left(\frac{P}{P_{std}}\right)^{-1/2}\right] \end{aligned} \qquad (8)$$

where $\Delta G_{f,H2O}$ and $\Delta G_{f,CO2}$ are the Gibbs free energy of formation for H_2O and CO_2, R is the ideal gas constant, and y_{O2} is the mole fraction of oxygen on the sweep side of the cells ($y_{O2} \sim 0.21$).

The electrolyzer outlet composition can be determined similarly, with one exception. The chemical balance equation for oxygen must be modified to account for the electrolytic reduction of the CO_2/steam mixture. Accordingly, the oxygen balance equation becomes:

$$a_1 + 2b_1 + d_1 = a_2 + 2b_2 + d_2 + \Delta n_O \qquad (9)$$

where Δn_O is the relative molar rate of oxygen removal from the CO_2 / steam mixture, give by:

$$\Delta n_O = \frac{I N_{cells}}{2 F \dot{N}_{Tot,fuel}} . \qquad (10)$$

In this equation, I is the electronic current, N_{cells} is the total number of cells in the stack, and $\dot{N}_{Tot,fuel}$ is the total molar flow rate on the CO_2/steam side, including any inert gas flows. So the post-electrolyzer equilibrium composition (state 2) can be determined again from simultaneous solution of three chemical balance equations and the equilibrium constant equation.

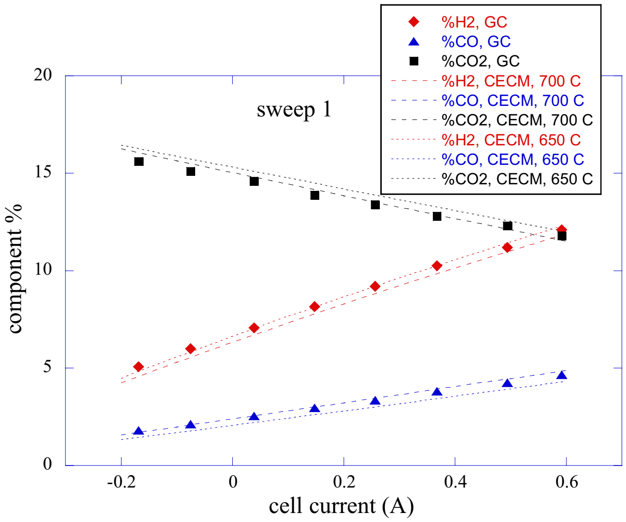

Fig. 10. Measured outlet gas compositions, with comparisons to predictions from the chemical equilibrium coelectrolysis model

The model was verified by comparing results with experimental results for various electrolysis current values, inlet compositions, and electrolysis temperatures.

SAMPLE BUTTON CELL TEST RESULTS

Open-cell potentials are monitored continuously during heatup as a system diagnostic. A significant departure of measured open-cell potentials from predicted values can indicate a problem such as a cracked cell or a short circuit. Electrolysis and coelectrolysis performance was characterized through a series of stepwise DC potential sweeps. Results of one such sweep are presented in Figure 10. The furnace temperature was 800°C. Inlet gas flow rates were 35 sccm N_2, 4 sccm H_2, 8 sccm CO_2, and 10.7 sccm H_2O. In Figure 10, the data symbols represent measurements obtained from the gas chromatograph. The lines represent predictions based upon a INL-developed chemical equilibrium coelectrolysis model (CECM). Two lines are shown for each case. The dashed lines represent CECM predictions based on an effective equilibrium temperature of 700°C. The dotted lines represent CECM predictions based on an effective equilibrium temperature of 650°C.

During coelectrolysis, the mole fractions of CO_2 and steam (not shown in Figure 10) decrease with current, while the mole fractions of H_2 and CO increase. For the conditions chosen for this test, the ratio of H_2 to CO is close to the desired 2-to-1 value for syngas production. Measured compositions of CO_2 and CO agree best with predictions based on an effective equilibrium temperature of 700°C. Measured compositions of H_2 agree best with predictions based on an effective equilibrium temperature of 650°C.

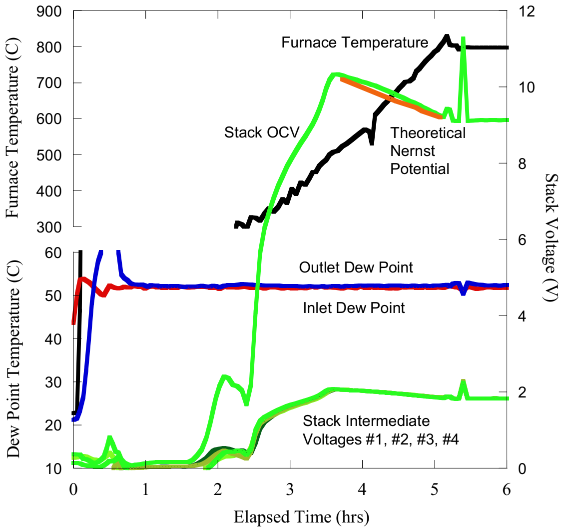

Fig. 11. Heat-up results for stack #1.

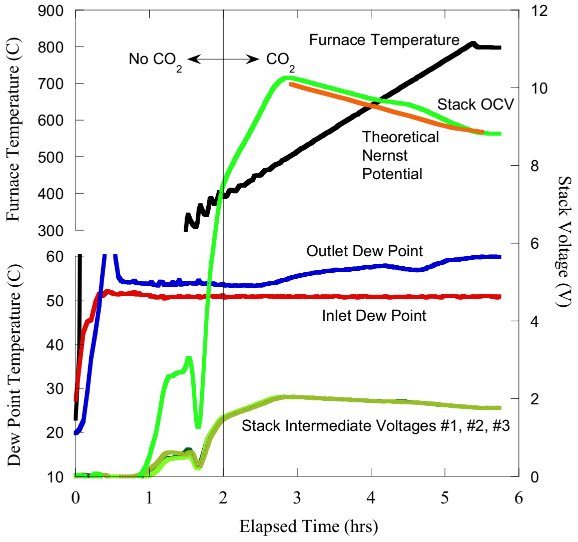

Fig. 12. Heat-up results for stack #2.

SAMPLE STACK TEST RESULTS

Within the past year, several 10-cell stacks were tested at the INL under steam and coelectrolysis conditions. The first two stacks were heated under identical initial conditions: 3000 sccm N_2 flow rate, 497 sccm H_2 flow rate, and an inlet gas dew point temperature of 51.8 C. However, in the case of stack #2, once all internal stack temperatures were above 350 C (or, after about 2 hours of heat up), 750 sccm of CO_2 was also introduced. Figures 11 and 12 show the heat-up profiles for stacks #1 and #2, respectively. Both stacks demonstrated remarkably similar heat-up profiles. The stacks do not exhibit an open cell potential (OCV) until above approximately 300-350 C, at which point the electrolyte begins to become an ion conductor. The orange lines represent the theoretical Nernst potentials for the gas mixtures, agreeing quite well with the measured OCVs. Of interest is that in the case of stack #2, the outlet dew point temperature begins to climb as the furnace temperature exceeds 450 C, indicating that the RSR has begun to reduce CO_2 and produce H_2O.

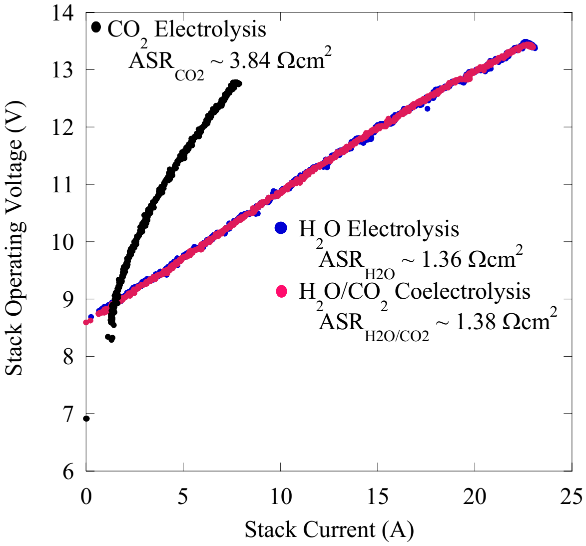

Fig. 13. Polarization curves for H_2O electrolysis, H_2O/CO_2 coelectrolysis versus CO_2 coelectrolysis, with mean ASR values.

Cell ASR is dependent upon the type of electrolysis being conducted, with pure CO_2 electrolysis exhibiting a significantly higher ASR than steam electrolysis. However, in coelectrolysis the RSR is probably relied upon for most CO_2-to-CO conversion, and steam electrolysis is the primary electrolytic reaction. Therefore, there is little change in ASR from steam electrolysis to coelectrolysis. To demonstrate this, polarization curves were generated for stack #3 for steam electrolysis, H_2O/CO_2 coelectrolysis, and CO_2 electrolysis. Once the stack was at the operating temperature of 800°C, a steam electrolysis polarization curve was generated by performing a voltage sweep for the conditions T = 800°C, H_2 = 996 sccm, CO_2 = 0 sccm, N_2 = 1009 sccm, with 54.8 mol% H_2O inlet. This same voltage sweep was repeated for coelectrolysis conditions T = 800°C, H_2 = 996 sccm, CO_2 = 1003 sccm, N_2 = 0 sccm, with 54.9 mol% H_2O inlet and for CO_2 electrolysis conditions T = 800°C, H_2 = 0 sccm, CO_2 = 1500 sccm, N_2 = 0 sccm, with 0 mol% H_2O inlet. These results are shown in Figure 13.

There was almost no change in apparent ASR for coelectrolysis versus steam electrolysis. However, the ASR for CO_2 electrolysis was significantly higher, reinforcing the hypothesis that steam electrolysis is the principal electrolysis reaction and that the RSR is mostly responsible for CO production.

Typical results of coelectrolysis sweep composition measurements are presented in Figure 14. This figure presents the compositions of steam, CO_2, hydrogen, and CO as a function of electrolysis current on a dry basis for stack #1. Conditions for this test were T = 800°C, H_2 = 497 sccm, CO_2 = 505 sccm, N_2 = 2510 sccm, with 11.4 mol% H_2O inlet. Lines

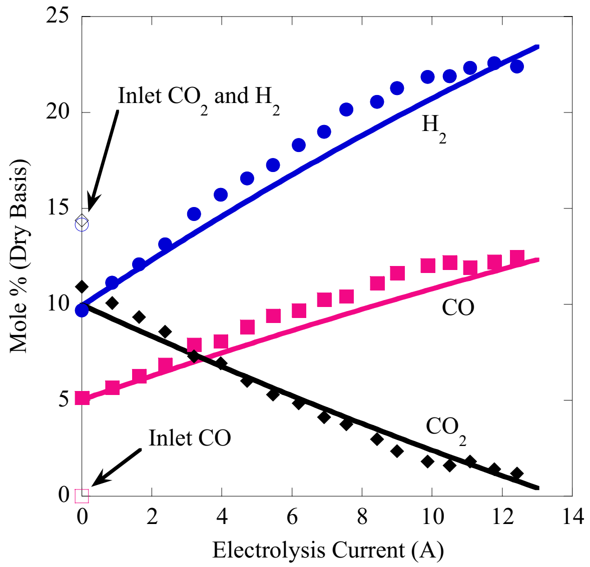

Fig. 14. Test 3 experimental and chemical equilibrium coelectrolysis model results, T_{equil} = 800 C.

represent model predictions and symbols represent experimental measurements. Figure 14 shows that even at zero current there was a drop in CO_2 and H_2 mole fractions from the cold inlet values, with CO produced. This is solely due to the RSR. As the electrolysis current was increased, the yield of syngas increased linearly while the concentration of CO_2 (and H_2O, not shown in the figures) decreased. Results also show overall good agreement between experimental GC data and results from the chemical equilibrium coelectrolysis model.

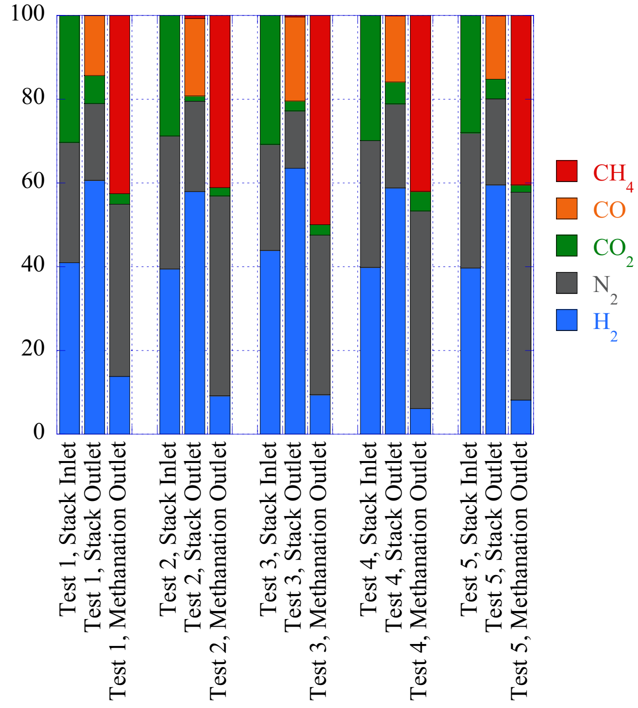

Fig 15. Coelectrolysis with subsequent methanation.

TABLE III.

Operating conditions for ILS module voltage sweep.

Hot zone temperature	820 C
Inlet water mass flow rate	34 ml/min
Inlet H_2 flow rate	5.4 Nl/min
Inlet N_2 flow rate	5.4 Nl/min
Inlet Air flow rate	25 Nl/min
Predicted OCV	50.5 V
Measured OCV	49.6 V
Predicted inlet dew point	90.3 C
Measured inlet dew point	91.3 C
Outlet dew point at OCV	90.2 C

Ceramatec Inc. extended their 10-cell stack testing apparatus by addition of a methanation reactor downstream of the stack. The methanation reactor consisted of a 18 mm inner diameter stainless steel tube, approximately 1.5 m in length. Within this tube was placed a commercial steam reforming catalyst (R-67R from Haldor Topsoe). This is a nickel catalyst on magnesium aluminate, a ceramic inert oxide of the spinel family. The reactor tube was placed within a zinc-aluminum sleeve to homogenize the axial temperature gradient. The reactor was maintained at approximately 300 C for testing. Testing consisted of high temperature coelectrolysis, with the coelectrolysis products immediately fed to the methanation reactor. Figure 15 summarizes the stack inlet, stack outlet, and methanation outlet stream compositions (volume %) for 5 tests. Between 40 and 50 volume % methane product was produced.

SAMPLE ILS TEST RESULTS

The INL ILS facility was first operated in the summer of 2007 with one 240 cell module in place. After heatup of the module, the facility was set at the operating conditions listed in Table III. The ILS module performance was tested by sweeping the module power supply voltage over the range of 50 to 79 V (0.83 V/cell to 1.32 V/cell). This range corresponds to operation from the open-cell voltage to slightly above the thermal neutral voltage. The corresponding voltage / current (VI) or polarization curve is displayed in Figure 16. The average per cell ASR for the initial ILS module, represented by the average slope of the VI curve, was measured to be 2.38 Ωcm^2. This value was significantly higher than the design value of 1.5 Ωcm^2, but was not unexpected. Subcontractor Cermatec Inc, the manufacturer of the ILS module, expected lower performance from this particular module due to manufacturing difficulties they had encountered. After testing samples of cells manufactured since this module, Ceramatec is certain that these problems have been solved and future modules should exhibit higher performance.

Stack internal temperatures initially decreased during the voltage sweep, due to the endothermic heat of reaction for water splitting. Once the operating voltage exceeded the thermal neutral voltage (77V for 60 cells), outlet gas temperatures exceeded inlet values.

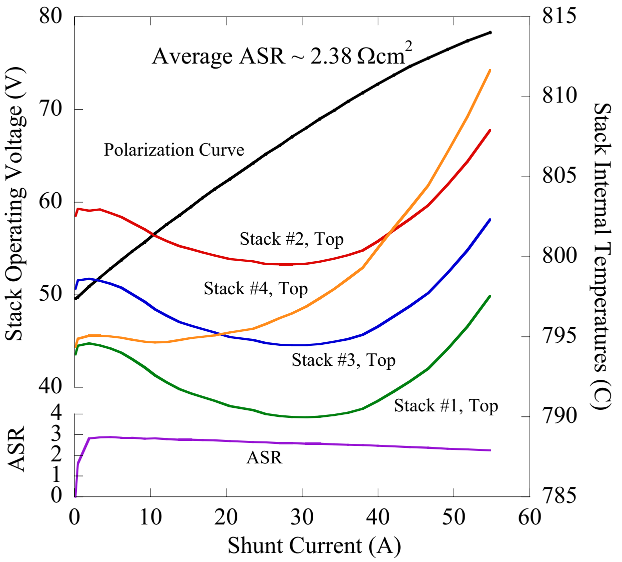

Fig. 16. ILS module voltage sweep / polarization curve.

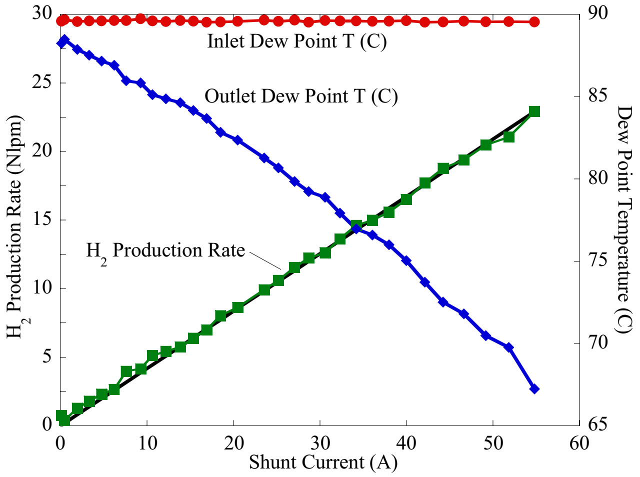

Fig. 17. ILS module voltage sweep hydrogen production rates and dew points.

Figure 17 presents inlet and outlet dewpoint temperatures and the hydrogen production rate for the ILS initial single-module sweep. The inlet gas dew point remained essentially constant at 89.6°C throughout the duration of the sweep. The outlet stream dew point temperature decreased continuously through the sweep as the operating voltage and stack current increased. The straight black line in Figure 17 represents the hydrogen production rate based on electrolysis current, while the green trace is the hydrogen production rate based on the difference between inlet and outlet dew points. Agreement between the two independent measurements of hydrogen production was generally excellent. At the highest current levels, H_2 production rates exceeded 1.4 Nm^3/hr (23 Nlpm).

CONCLUSIONS

The INL, in collaboration with Ceramatec Inc., has been actively researching the use of solid oxide cells for high temperature electrolysis of steam for H_2 production and steam/CO_2 for syngas production. Testing has been conducted at various scales, including button cell (~1 W), stack (~200 W), and the INL ILS facility (5 kW, ultimately 15 kW). Testing has shown high temperature electrolysis to be a promising technology for efficient large-scale production of H_2 and/or syngas.

ACKNOWLEDGMENTS

This work was supported by the U.S. Department of Energy, Office of Nuclear Energy, Nuclear Hydrogen Initiative Program. The Idaho National Laboratory is operated for the U.S. Department of Energy's Office of Nuclear Energy by the Battelle Energy Alliance under contract number DE-AC07-05ID14517.

REFERENCES

[1] Hirsch, R. L., Bezdek, R., and Wendling, R., "Peaking of World Oil Production: Impacts, Mitigation, & Risk Management," DOE NETL, February, 2005.

[2] Sandalow, D., *Freedom From Oil*, McGraw-Hill , New York, 2008.

[3] Yildiz, B., and Kazimi, M. S., "Nuclear Energy Options for Hydrogen and Hydrogen-Based Liquid Fuels Production," MIT-NES-TR-001, September 2003.

[4] Condie, K.G., Stoots, C.M., O'Brien, J.E., and Herring, J.S., "Characterization of the Transient Response of the ILS with One Module Installed to Heatup Changes in Power Level and Cooldown," INL Technical Report INL/EXT-07-13626, December, 2007.

[5] O'Brien, J. E., Stoots, C. M., Herring, J. S., and Hartvigsen, J. J.,"Hydrogen Production Performance of a 10-Cell Planar Solid-Oxide Electrolysis Stack," *Journal of Fuel Cell Science and Technology*, **3**, pp. 213-219, (2006).

[6] Herring, J. S., O'Brien, J. E., Stoots, C. M., and Hawkes, G. L., "Progress in High-Temperature Electrolysis for Hydrogen Production using Planar SOFC Technology," *International Journal of Hydrogen Energy*, **32**, *4*, pp. 440-450 (2007).

[7] Stoots, C. M., O'Brien, J. E., McKellar, M. G., Hawkes, G. L., and Herring, J. S., "Engineering Process Model for High-Temperature Steam Electrolysis System Performance Evaluation," *Proc. of the AIChE 2005 Annual Meeting*, Cincinnati, Oct. 30 – Nov. 4, 2005.